4490

Intra- and Inter-scanner Variability Evaluation of RR-VFA B1+ and T1 in the Prostate at 3T

Xinran Zhong[1,2], Dapeng Liu[1], James Sayre[1], Holden H Wu[1,2], and Kyunghyun Sung[1,2]

[1]*Department of Radiological Sciences, University of California, Los Angeles, Los Angeles, CA, United States,* [2]*Physics and Biology in Medicine IDP, University of California, Los Angeles, Los Angeles, CA, United States*

Synopsis

Accurate T_1 estimation is critical for quantitative prostate DCE MRI. B_1^+ inhomogeneity can introduce significant error into the T_1 quantification, especially for variable flip angle method. Reference region variable flip angle (RR-VFA) method is a promising B_1^+ and T_1 estimation technique, which requires no separate scans for B_1^+ mapping and can reduce slice profile and position mismatch between B_1^+ and T_1 maps. In this study, we investigated both intra-scanner repeatability and inter-scanner reproducibility regarding B_1^+ corrected T_1 on two 3.0 T scanners to compare RR-VFA to a commercially available B_1^+ estimation technique. RR-VFA showed comparable intra- and inter-scanner variability to the saturated turbo FLASH based B_1^+ estimation technique.

INTRODUCTION

Quantitative dynamic contrast-enhanced (DCE) MRI is a widely used tool for prostate cancer diagnosis[1]. The quantitative analysis of DCE-MRI typically requires accurate estimation of pre-contrast T_1, where the variable flip angle (VFA) method is commonly used[2]. However, the VFA method is sensitive to B_1^+ inhomogeneity, which can introduce error into the prescribed flip angles and subsequent T_1 quantification.[3] The reference region VFA (RR-VFA) method is a promising B_1^+ and T_1 estimation technique[4,5], which has potential to improve clinical prostate quantitative DCE estimation because it does not require a separate scan for B_1^+ mapping and can reduce slice profile and position mismatch between B_1^+ and T_1 maps. In this work, we compared the RR-VFA technique to a commercially available B_1^+ estimation techniques based on saturated turbo FLASH (satTFL)[6] regarding intra- and inter-scanner variability of B_1^+ corrected T_1 maps.

METHODS

With IRB approval, ten healthy male subjects with mean age of 29.3±4.2 years old were prospectively recruited in this study with written informed consent. Each subject was scanned on two different 3.0T systems Prisma ("Scanner 1") and Skyra ("Scanner 2") (Siemens Healthcare, Erlangen, Germany) respectively. On each scanner, each subject was scanned twice in the feet-first supine position, with repositioning between the two scans. The general workflow is shown in Fig. 1. The protocol included 2D T_2 weighted Turbo Spin Echo (T2W TSE), 2D saturated turbo FLASH (satTFL) B_1^+ sequence and 3D VFA imaging with a dual echo bipolar readout (TEs=1.23/2.46 ms). The body coil was used for RF transmission and a receive-only phased array coil was used for signal reception. "TrueForm" B_1^+ shimming mode was active for both scanners.[7]

Relative flip angle maps (obtained flip angle/prescribed flip angle×100%) were generated using both RR-VFA and satTFL. Three T_1 maps (T_1 without B_1^+ correction, satTFL corrected T_1 and RR-VFA corrected T_1) were calculated for each scan. Regions of interests (ROI) were positioned on three representative slices (base, mid and apex) in the prostate, as well as the left and right obturator internus muscles, on each T2W TSE scan. We matched the slices manually between scans. For each scan, two B_1^+ maps and three T_1 maps were estimated, and both B_1^+ and T_1 maps were linearly interpolated to the same dimension as the 2D T2W TSE acquisition so that the ROI drawn on T2W TSE scans could be transferred to those maps directly. All post-processing was performed using in-house scripts written in Matlab (Mathworks, Natick, Mass).

B_1^+ estimations from two methods within each ROI were compared using linear regression and Pearson's correlation. The Pearson's correlation was also used to compare T_1 between scans for intra- and inter-scanner variability evaluation. For intra-scanner variability, the average T_1 between the two scans on the same scanner for the same volunteer were compared using paired t-test, Linear Regression and Bland Altman plot. Similarly, inter-scanner variability was assessed by determining the correlation and agreement of the average T_1 between the scans of two different systems for the same volunteer.

RESULTS and DISCUSSION

Representative ROI positioning for three T_1 maps from the same scan is shown in Fig. 2. The uncorrected T_1 shows inconsistent T_1 values between left and right obturator internus muscles, and the inconsistency is reduced in both B_1^+ corrected T_1 maps.

Linear regression between average B_1^+ from RR-VFA and satTFL gives a slope of 1.2 when comparing RR-VFA to satTFL B_1^+. The squared Pearson correlation coefficient (r^2) between two B_1^+ estimation techniques is 0.859, showing good linear correlation.

Evaluation of T_1 using paired t-test is shown in Fig 3. T_1 from different scans before B_1^+ correction is significantly different from each other, while not significantly different after B_1^+ correction using both B_1^+ estimation methods. Also, the intra- and inter-scanner comparison of linear regression is shown in Fig. 4. A higher squared Pearson Correlation (r^2) is observed in RR-VFA corrected T_1 compared to uncorrected T_1 and satTFL corrected T_1. The intra-and inter-scanner comparison of Bland-Altman plot is shown in Fig. 5. The 95% limits of agreement for RR-VFA corrected T_1 is smaller than that of uncorrected T_1 as well as satTFL corrected T_1.

CONCLUSION

The intra- and inter-scanner variability of T_1 estimation has been significantly reduced using both RR-VFA and satTFL. The RR-VFA corrected T_1 had similar intra- and inter-scanner variability to the satTFL corrected T_1, and RR-VFA provides B_1^+ estimation highly correlated to satTFL ($r^2 = 0.859$). Considering other advantages of RR-VFA such as no requirement for a separate scan, RR-VFA shows great potential in improving the prostate quantitative DCE-MRI.

Acknowledgements

No acknowledgement found.

References

1. Alonzi R, Padhani AR, Allen C. Dynamic contrast enhanced MRI in prostate cancer. European Journal of Radiology. 2007;63(3):335–350. doi:10.1016/j.ejrad.2007.06.028 2

2. Gupta RK. A new look at the method of variable nutation angle for the measurement of spin-lattice relaxation times using fourier transform NMR. Journal of Magnetic Resonance. 1977;25(1):231–235. doi:10.1016/0022-2364(77)90138-X

3. Sung K, Daniel BL, Hargreaves BA. Transmit B1+ field inhomogeneity and T1 estimation errors in breast DCE-MRI at 3 tesla. Journal of magnetic resonance imaging : JMRI. 2013;38(2):454–9. doi:10.1002/jmri.23996

4. Sung K, Saranathan M, Daniel BL, Hargreaves BA. Simultaneous T 1 and B 1 + Mapping Using Reference Region Variable Flip Angle Imaging. Magnetic Resonance in Medicine. 2013;70(4):954–961. http://doi.wiley.com/10.1002/mrm.24904. doi:10.1002/mrm.24904

5. Rangwala NA, Dregely I, Wu HH, Sung K. Optimization and evaluation of reference region variable flip angle (RR-VFA) B1+ and T1 Mapping in the Prostate at 3T. Journal of Magnetic Resonance Imaging. 2017;45(3):751–760. doi:10.1002/jmri.25410

6. Chung S, Kim D, Breton E, Axel L. Rapid B1+ mapping using a preconditioning RF pulse with turboFLASH readout. Magnetic Resonance in Medicine. 2010;64(2):439–446. http://doi.wiley.com/10.1002/mrm.22423. doi:10.1002/mrm.22423

7. Blasche M, Riffel P, Matthias L. TimTX TrueShape and syngo ZOOMit technical and practical aspects. MAGNETOM Flash 2012:74–84. 39.

Figures

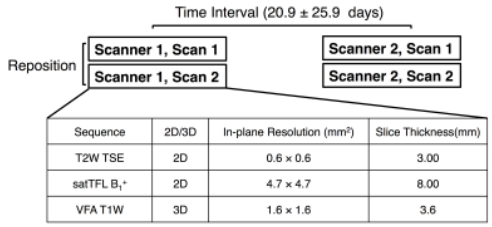

Sequence	2D/3D	In-plane Resolution (mm²)	Slice Thickness(mm)
T2W TSE	2D	0.6 × 0.6	3.00
satTFL B_1^+	2D	4.7 × 4.7	8.00
VFA T1W	3D	1.6 × 1.6	3.6

Figure 1. Workflow and protocols for the experiment. Each volunteer was scanned four times on two 3.0 T scanners.

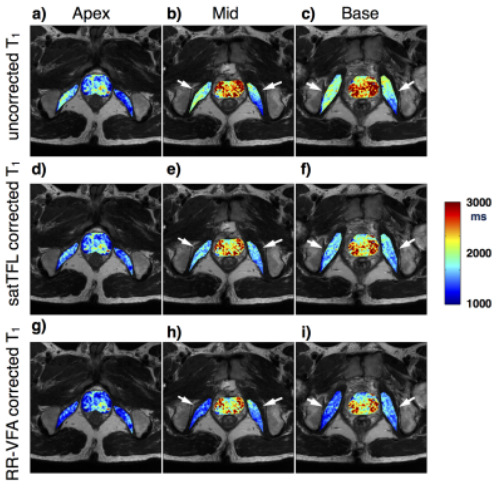

Figure 2. T_1 value within ROIs overlaid on T2W-TSE image. Three ROIs for obturator internus muscles and the prostate region were positioned on three selected slices respectively for each scan. The inconsistent T_1 between left and right muscles is reduced after B_1^+ correction using either method (marked by white arrow).

p-value (2-tailed)	Intra-Scanner		Inter-Scanner
	Scanner 1	Scanner 2	
Uncorrected T_1	0.039*	0.044*	0.000*
satTFL corrected T_1	0.070	0.587	0.162
RR-VFA corrected T_1	0.158	0.918	0.394

Figure 3. Paired t-test results between average T_1 within ROIs for both intra-and inter scanner comparison. The T_1s between different scans are significantly different (marked by *) before B_1^+ correction and become not significantly different after correction using B_1^+ correction with two B_1^+ estimation techniques.

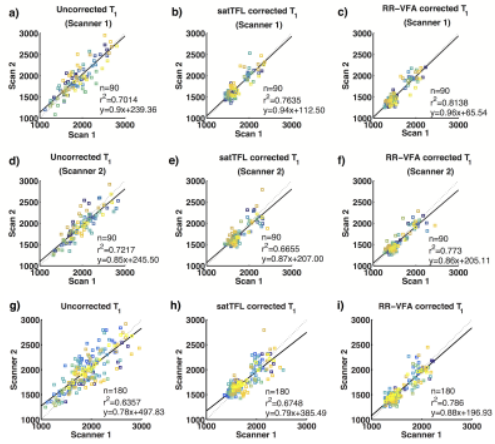

Figure 4. Linear Regression and squared Pearson's Correlation (r^2) for both intra-scanner comparison (a-f) and inter-scanner comparison (g-i) between average T_1 within each ROI between scans. Each encoded color indicates one volunteer. RR-VFA corrected T_1 has the highest r^2.

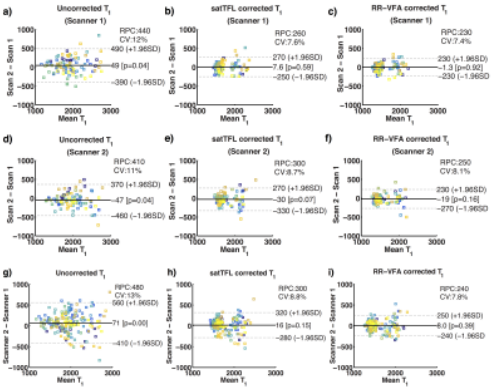

Figure 5. Bland-Altman plots for both intra-scanner comparison (a-f) and inter-scanner comparison (g-i) to show the agreement of average T_1 within each ROI between scans. Each encoded color indicates one volunteer. RR-VFA corrected T_1 has the smallest 95% limits of agreement.